Paleolimnological features of a mega-lake phase in the Makgadikgadi Basin (Kalahari, Botswana) during Marine Isotope Stage 5 inferred from diatoms

Mareike Schmidt • Markus Fuchs • Andrew C. G. Henderson • Annette Kossler • Melanie J. Leng • Anson W. Mackay • Elisha Shemang • Frank Riedel

M. Schmidt, A. Kossler, F. Riedel (✉)
Institute of Geological Sciences, Freie Universität Berlin, Malteserstr. 74-100, 12249 Berlin, Germany
e-mail: paleobio@zedat.fu-berlin.de

M. Fuchs
Department of Geography, Universität Gießen, Senckenbergstr. 1, 35390 Gießen, Germany

A. C. G. Henderson
School of Geography, Politics and Sociology, Newcastle University, Newcastle upon Tyne, NE1 7RU, UK

M. J. Leng
NERC Isotope Geosciences Facility, British Geological Survey, Nottingham NG12 5GG, UK and Centre for Environmental Geochemistry, University of Nottingham, Nottingham NG7 2RD, UK

A. W. Mackay

Environmental Change Research Centre, Department of Geography, UCL, Gower Street, London, WC1E 6BT, UK

E. Shemang
Department of Earth and Environmental Sciences, Botswana International University of Science and Technology, Palapye, P. Bag 16, Botswana

Keywords

Late Pleistocene, southern Africa, Lake Palaeo-Makgadikgadi highstand, diatoms, stable oxygen isotopes, Heinrich event

Abstract

The Makgadikgadi-Okavango-Zambezi basin (MOZB) is a structural depression in the south-western branch of the East African Rift System of the northern and middle Kalahari, central southern Africa. In the present day, the mainly dry subbasins of the MOZB are part of a long-lived lacustrine system that has likely existed since Early Pleistocene and from which an extant freshwater fish radiation emerged seeding all major river systems of southern Africa. During hydrologically favourable periods the subbasins were connected as a single mega-lake termed Lake Palaeo-Makgadikgadi. Previous geomorphological studies and OSL dates have provided evidence for repeated mega-lake periods since approximately 300 ka. The environmental and climatic implications of such large scale late Quaternary lake-level fluctuations are controversial, with the duration of mega-lake phases poorly constrained.

Here, we present the first evidence for a Marine Isotope Stage (MIS) 5 mega-lake period (about 935-940 m a.s.l.) reconstructed from a diatom-rich, 30-cm-thick lacustrine sediment

section, exposed close to a palaeo-shoreline of the Makgadikgadi Basin. Based upon the environmental setting and in comparison with sedimentation rates of other similar lake environments, we tentatively estimated that the highstand lasted approximately 1 ka during MIS 5d-b. The 30-cm section was sampled in 0.5-cm steps. Diatom species diversity ranges from 19 to 30 through the section. The dominant species are *Pseudostaurosira brevistriata*, *Rhopalodia gibberula*, *Cyclotella meneghiniana* and *Epithemia sorex*. The total of 60 sediment samples provide us with a record at decadal to bi-decadal resolution. Based on diatom assemblages and their oxygen isotope composition ($\delta^{18}O$) we infer an alkaline and mostly oligohaline lake with shallow water conditions prevailing in MIS 5, and is potentially analogous to a Heinrich event. The climate over southern Africa during MIS 5 has been considered very arid but the hydromorphological context of our sediment section indicates that we captured a mega-lake period providing evidence that short-term excursions to significantly higher humidity existed. A hydrologically more favourable environment during MIS 5 than formerly presumed is in line with the early human occupation of the Kalahari.

Introduction

Geomorphological studies of the northern and middle Kalahari in northern Botswana have provided evidence of a former mega-lake system (Passarge 1904; Grove 1969; Ebert and Hitchcock 1978; Cooke 1979; Heine 1982; Thomas and Shaw 1991; Burrough et al. 2009a; Podgorski et al. 2013; Riedel et al. 2014; Fig. 1), which developed within the Makgadikgadi-Okavango-Zambezi basin (MOZB). The structural depression of the MOZB belongs to the south-western branch of the East African Rift System (Ringrose et al. 2005; Kinabo et al. 2007; Shemang and Molwalefhe 2011; Riedel et al. 2014). Grey and Cooke (1977) termed highstands in this lacustrine system Lake Palaeo-Makgadikgadi (referring to the Makgadikgadi Basin, the largest and deepest of the depressions), which likely comprised of several lacustrine basins (Fig.

78 1) and exhibited a maximum expansion of about 66,000-90,000 km^2 (Eckardt et al. 2008;
79 Podgorski et al. 2013). There is geological and phylogeographical evidence that the mega-lake
80 system may have existed since the Early Pleistocene (Genner et al. 2007; Moore et al. 2012;
81 Riedel et al. 2014; Schultheiß et al. 2014). An OSL (optical stimulated luminescence) date of
82 *c.* 290 ka (Burrough et al. 2009a) provides only a minimum age of the palaeolake system as this
83 is at the limit of the OSL dating technique (Cordier et al. 2012).

84 Burrough et al. (2009a) presented a large number of OSL dates in order to illuminate
85 the chronology of mega-lake periods. Apart from two dates that fall within MIS 8 (*c.* 290 ka
86 and *c.* 270 ka) they dated highstands during MIS 5 to MIS 1. Their OSL samples were taken
87 from palaeo-shorelines of the Makgadikgadi Basin which represents the dominant water body
88 during Lake Palaeo-Makgadikgadi highstands. Burrough et al. (2009a) inferred seven periods
89 of lake highstands in the Makgadikgadi Basin during the past approximately 105 ka. Two of
90 these occurred during MIS 5 (104.6 ± 3.1 ka and 92.2 ± 1.5 ka) and the next youngest one is of
91 MIS 4 age (64.2 ± 2.0 ka).

92 Today, the Makgadikgadi Basin (Fig. 1) is characterized by several salt pans. The largest
93 are the central Ntwetwe Pan (about 4700 km^2) and the eastern Sua Pan (about 3000 km^2), which
94 are occasionally filled with water in modern times, but these temporary infills are not high
95 enough to link the pans together (Riedel et al. 2012). The bottoms of the pans lie generally
96 below an altitude of 950 m a.s.l. (Grove 1969; Grey and Cooke 1977; Cooke 1980; Mallick et
97 al. 1981), with the deepest point (also of the MOZB) located in the northern part of the Sua Pan
98 at an altitude of 890 m a.s.l. (Cooke 1980; Thomas and Shaw 1991; Eckardt et al. 2008).

99 The western margin of the Makgadikgadi Basin is sharply bordered by the prominent
100 Gidikwe Ridge (Fig. 1), which stretches about 250 km from north to south and exhibits a series
101 of palaeo-shorelines. Here, two distinct palaeo-shorelines were determined at an altitude of 945
102 and 936 m a.s.l. (Cooke and Verstappen 1984; Thomas and Shaw 1991; Burrough et al. 2009a,
103 2009b). Lacustrine sediments recorded west to the Gidikwe Ridge (Fig. 1) were interpreted to

104 be of lagoon origin (Cooke 1980; Thomas and Shaw 1991). The backside of the Gidikwe Ridge,
105 however, was considered a second ridge (Moremaoto) by Gumbricht et al. (2001; personal
106 observations FR), delimiting the Makalamabedi Basin (Fig. 1) to the east, which exhibits a
107 curvilinear morphology interpreted as palaeo-shorelines at approximately 930-940 m a.s.l.
108 (Gumbricht et al. 2001; Riedel et al. 2014). Near the Moremaoto Ridge about 2-m-thick diatom-
109 rich sediments (personal observation MS and FR) are exposed, which were originally described
110 in Passarge (1904) who considered an Eemian (MIS 5e) lake period. Shaw et al. (1997) re-
111 studied the diatom-rich sediments, established a MIS 3 age and related them to a lake highstand
112 of the Makgadikgadi Basin. These sediments however are located in the Makalamabedi Basin
113 (Riedel et al. 2014).

114 There are currently no palaeontological records from lacustrine sediments in the MOZB
115 older than MIS 3 (Riedel et al. 2014) that could be used to characterise mega-lake periods.
116 Joyce et al. (2005) concluded an extant cichlid radiation emerged from Lake Palaeo-
117 Makgadikgadi during the Middle Pleistocene seeding all major river systems of southern
118 Africa. These fish require freshwater habitats, which could be sustained over longer periods
119 only when the lake had an outlet (Riedel et al. 2014). The Zambezi, which transverses the
120 northern extension of the lacustrine system, could have acted as an outflow during highstands
121 when all basins where connected into a single mega-lake. It has been suggested that the inflow
122 of the Okavango River, and possibly of the Zambezi, controlled mega-lake periods (Nugent
123 1990). There are, however, several fossil river systems entering the Makgadikgadi Basin
124 (Riedel et al. 2014) of which the Okwa Valley is the largest (Fig. 1). Riedel et al. (2014)
125 suggested that the Okwa River was fully active for the last time during the Last Glacial
126 Maximum and ceased flowing during Heinrich event 1. So far it can only be speculated whether
127 during periods of enhanced Okwa River inflow the Makgadikgadi Basin became exorheic, with
128 an outflow to the west, and freshwater conditions prevailed (Riedel et al. 2014).

129 On the one hand the environmental and climatic implications of such large scale late
130 Quaternary lake-level fluctuations and the dynamics of aeolian activity are mainly controversial
131 and on the other hand the discussion has focussed especially on the period MIS 3 to MIS 1
132 (Street and Grove 1976; van Zinderen Bakker 1976; Heine 1981, 1987, 1988; Stokes et al. 1997;
133 Gasse et al. 2008; Burrough and Thomas 2009; Burrough et al. 2009a, 2009b; Hürkamp et al.
134 2011; Riedel et al. 2014). There has been limited work on MIS 5 sediments, and some climate
135 interpretations do exist although these rely heavily on marine sediments (from off Namibia: Shi
136 et al. 2001; Stuut et al. 2002) at a low temporal resolution (Urrego et al. 2015). It is noteworthy
137 that Urrego et al. (2015) reported increased aridity in south-western Africa (neighboring our
138 study area) during the warmest periods of MIS 5 (5e, 5c, 5a), but they also identified short
139 increases in humidity during warm-cold and cold-warm transitions. Geyh and Heine (2014)
140 reported MIS 5 speleothem growth from the Namib Desert. In south-eastern Africa, MIS 5 was
141 characterized by episodes of extremely arid conditions leading to dramatic lowstands of Lake
142 Malawi (Cohen et al. 2007; Scholz et al. 2007).
143 These tropical African MIS 5 "megadroughts" (Scholz et al. 2007) are discussed to have
144 facilitated human expansions across Africa and ultimately out of Africa (Rito et al. 2013).
145 Genetic data suggest that anatomically modern humans (Balter 2002) originated in Africa
146 during MIS 6 (Ingman et al. 2000) and there is archaeological evidence that they populated the
147 southern tip of Africa as early as ~165 ka (Marean et al. 2007). Genomic diversity of extant
148 hunter-gatherer populations is in agreement with this early occupation of southern Africa and
149 tentatively suggests even the orgin of modern humans from this region (Henn et al. 2011).
150 Symbolic and thus modern behaviour of such southern African human populations may have
151 first appeared during MIS 5a (Henshilwood et al. 2002) or early MIS 4 (Jacobs and Roberts
152 2009). In the Kalahari, archaeological sites at the Tsodilo Hills indicate human occupation since
153 at least 90 ka (Robbins et al. 2016). Burrough (2016) discussed the environmental contributions

154 to early human dispersal in the Kalahari and emphasised the contrast between MIS 5 lake
155 highstands in the Makgadikgadi Basin and extreme lowstands of Lake Malawi.
156 The modern climate setting over semi-arid southern Africa is complex (Peel et al. 2007;
157 Gasse et al. 2008; Chase et al. 2012; Riedel et al. 2014) and comprises moisture transport from
158 the West and East African monsoons (including convective moisture from the Congo Basin) to
159 the Okavango catchment and the Kalahari during austral summer. Rainfall variability in
160 Botswana is described by Batisami and Yarnal (2010).During austral winter, moisture from the
161 south-eastern Atlantic triggers rainfall (mainly) over the Western Cape Province. South-western
162 Indian Ocean (Agulhas Current) derived moisture triggers rainfall over southern Africa mainly
163 during austral summer but also during winter (Chase and Meadows 2007; Gasse et al. 2008;
164 Burrough et al. 2009b; Chase et al. 2012; Urrego et al. 2015).
165 The aim of our study is to reconstruct for the first time the palaeohydrological status of
166 a mega-lake phase (about 66,000-90,000 km^2) in the MOZB, which corresponds to a highstand
167 of at least 936-945 m a.s.l. of Lake Palaeo-Makgadikgadi, by analyzing diatom assemblages
168 and their oxygen isotope composition ($\delta^{18}O_{diatom}$). The mega-lake phase adressed here occurred
169 during MIS 5 and is the first attempt to infer the duration of a mega-lake phase in this region.
170 Our findings contribute to the understanding of phylogeographical patterns and climate
171 evolution of southern Africa.
172
173 Study site
174
175 Our study site (Fig. 1) is located at the Gidikwe Ridge where the ridge is cut by the Boteti River
176 valley forming a 20-22 m deep gorge. Here, a 10-m-thick sedimentary succession was exposed
177 (S20.28672°, E24.26822°), which exhibited 40 cm consolidated, heavily diagenetically altered
178 lacustrine deposits at the base, followed by 9.3 m unfossiliferous, silcrete- and calcrete-rich
179 playa sediments (Riedel et al. 2014). On the top of the succession of sediments, at about 935 m

180 a.s.l., the playa sediments are overlain by a 30-cm-thick unit (Fig. 2), which consists of
181 consolidated, fine-laminated to thin-bedded, finely clastic, light-grey to whitish lacustrine
182 sediments rich in diatoms and deposited during MIS 5 (Riedel et al. 2014). Lithological hiatuses
183 were not identified in the 30-cm unit, suggesting sedimentation was continuous. This sediment
184 unit thins out a few hundred metres west of the section where sandy palaeo-beach features can
185 be found indicating that the former shore was relatively close.
186
187 **Material and Methods**
188
189 Sediment samples
190
191 The 10-m sediment outcrop within the Boteti Gorge at the western margin of the Makgadikgadi
192 Basin (Fig. 1 and 2) was first visited by AK and FR in 2007 and a small number of samples
193 were taken. Samples from a 40-cm-thick unit of white and pale-gray lacustrine sediments at the
194 base of the profile has been strongly affected by diagenesis, and contains only few broken
195 valves of diatoms, while the light-grey to whitish 30-cm-thick deposits at the top of the section
196 (Boteti Top = BT) have abundant diatoms. Although carbonate is contained in BT, remains of
197 ostracod valves were only exceptionally preserved. Except for a few pollen grains, no other
198 fossil remains were identified. When revisiting the section in 2009 samples for OSL dating
199 were taken from the two lacustrine sediment units. MF provided an OSL date suggesting MIS
200 5 age for BT. OSL dating of the 40-cm unit at the base of the Boteti section failed because the
201 OSL signal was close to saturation and therefore at its upper limit.
202 In 2011 the outcrop was revisited for high resolution sampling and a fresh surface was
203 exposed and thoroughly cleaned using spade, saw, knife and brush. The sampling of the
204 relatively hard sediments was done in 0.5-cm increments with a knife from the base to the top
205 of the BT unit. 60 sediment samples of about 60 grams each were taken, sample BT_{diatom}-1

206 corresponding to the lowermost and sample BT_{diatom}-60 to the uppermost layer. In addition,
207 using a saw, a 30x15x15-cm-sediment block was removed covering the complete BT unit in
208 order to obtain suitable material for optical dating. The sawed surfaces did not exhibit cracks
209 through which light could have penetrated into the internal sediments. The block was
210 immediately wrapped with thick black plastic foil and stored in a sealed box.
211
212 OSL dating
213
214 Samples were taken from the lower (BT 1055), middle (BT 1054) and upper part (BT 1052) of
215 the sediment block in the OSL lab of Bayreuth University, Germany. A further sample (BT
216 885) from the middle part of the BT section had been already obtained during field work in
217 2009 (Fig. 2).
218 The coarse grain quartz fraction (90-200 μm) of the sediment samples was used for OSL
219 dating. Luminescence measurements were carried out using a Risø-Reader TL/OSL-DA-15
220 (Bøtter-Jensen 1997), equipped with blue LEDs (470 ± 30 nm) for stimulation, a Thorn-EMI
221 9235QA photomultiplier combined with one 7.5 mm U-340 Hoya filter (transmission 290-370
222 nm) for detection and a $^{90}Y/^{90}Sr$ β-source (8.1 ± 0.6 Gy/min) for artificial irradiation.
223 The equivalent dose (D_e) was determined by applying a single aliquot regenerative
224 (SAR) dose protocol (Murray and Wintle 2000). Shine-down curves were measured for 20 s at
225 elevated temperatures (125°C) after a preheat for 10 s at 220°C and 240°C respectively for the
226 natural and regenerated signals and a cut-heat of 160°C for the test doses. The preheat
227 temperatures were chosen after a preheat plateau test, which indicated that the given dose could
228 be reproduced within a temperature range of 220°C to 240°C.
229 Finally, the D_e was calculated from the integral of the first 0.4 s from the shine-down
230 curves after subtracting the mean background (16-20 s) signal. For each sample, up to 28 small
231 aliquots (steal cups) were measured with 200-500 grains per aliquot. Possible feldspar

232 contamination of the aliquots was checked by stimulating the artificially irradiated samples with
233 infrared (IR-OSL) and detecting in the UV range (290-370 nm). For D_e determination, only
234 those aliquots of a sample were used, which passed the criteria of a recycling ratio of 1 ± 0.1
235 and a recuperation value of < 5% (Murray and Wintle 2000). The standard error was used as D_e
236 error.

237 The dose rate($\dot{D}$) for OSL age calculation was determined by thick source α-counting
238 and ICP-MS. Cosmic-ray dose rates were calculated according to Prescott and Hutton (1994).
239 The water content of the samples was determined using the average value of the possible water
240 content range, based on the porosity of the samples. An error for the water content value was
241 chosen, which included the possible water content range. The values used for the water content
242 were checked by measuring the in situ water contents of the samples, showing conformity
243 within errors.

244

245 Diatom assemblages

246

247 Diatom extraction and slide preparation for microscopic analyses were carried out following
248 Battarbee et al. (2001). Diatom identification and counting were performed using a Meiji
249 Techno 4000 microscope at 1000x magnification with an oil immersion objective.
250 Approximately 500 diatom valves were counted per sample to ensure that effective numbers of
251 taxa were counted. Diatom relative abundances were plotted using Tilia® (Grimm 1991-2011),
252 and planktonic to benthic ratios calculated according to the formula: ∑(planktonic) /
253 ∑(planktonic + benthic).

254 For precise identification of the diatom taxa, a Zeiss Supra 40 VP scanning electron
255 microscope (SEM) was additionally used. Diatoms for the SEM analyses were prepared by
256 drying 0.5 ml of the treated sample suspension on a cover slip fixed on a stub. After drying, the
257 diatoms were coated with gold in a sputter coater and then examined with the SEM. Diatom

258 species were identified using, amongst other keys, Krammer (2002), Krammer and Lange-
259 Bertalot (1997, 1999, 2000, 2004), Levkov (2009) and Kusber and Cocquyt (2012). A list of
260 species and their authorities is provided in ESM 1.

261 The ecological preferences of identified diatoms concerning salinity, pH and trophic
262 level were taken from the literature (ESM 2), but are unknown in some taxa. The salinity
263 classification follows Schlungbaum and Baudler (2001): freshwater = < 0.5 psu; oligohaline =
264 0.5 to < 5 psu; mesohaline = 5 to 18 psu; euryhaline = fresh to saltwater, indifferent or non-
265 significant.

266 Ordination analyses were undertaken using Canoco 4.5 (ter Braak and Šmilauer 2002)
267 to reveal major trends in the diatom data. An initial detrended correspondence analysis (DCA)
268 gave an axis 1 gradient of only 0.734, revealing a dataset with very little species turnover, so
269 principal components analysis (PCA) was used instead. Scaling for both samples and species
270 was optimized through symmetric scaling of the ordination scores (Gabriel 2002). Because we
271 have closed relative abundance data, species data were log (x+1) transformed and both species
272 and samples were centred to give a log-linear contrast PCA (Lotter and Birks 1993). To
273 determine if any of the PCA axes were in themselves significant in explaining variation in the
274 diatom data, a broken stick analyses was undertaken (Jollifer 1986). The diatom stratigraphy
275 was zoned using Constrained Incremental Sum of Squares Cluster Analysis (CONISS)
276 according to Grimm (1991-2011).

277

278 Diatom oxygen isotope analysis

279

280 From the 60 BT samples studied in respect of diatom assemblages, alternate samples were
281 analysed for their oxygen isotope composition. Following the protocol established by Morley
282 et al. (2004) the 30 sediment samples for $\delta^{18}O_{diatom}$ analysis underwent chemical digestion using
283 30% H_2O_2 and 5% HCl followed by sieving of samples at 74 μm and 10 μm. Diatoms were

284 then isolated using a combination of differential settling and heavy liquid separation using
285 sodium polytungstate (SPT). The SPT was then washed out of the purified sample using
286 multiple rinses of deionised distilled water, and dried down prior to analysis. Samples were
287 measured using a step-wise fluorination procedure using 6 mg of sample (Leng and Sloane
288 2008) and a Finnigan MAT 253 isotope ratio mass spectrometer. $\delta^{18}O_{diatom}$ were converted to
289 the Vienna Standard Mean Ocean Water (VSMOW) scale using an international laboratory
290 diatom standard (BFC_{mod}) calibrated against NBS28. The methology has been verified through
291 an inter-laboratory calibration exercise (Chapligin et al. 2011). Replicate analyses of sample
292 material from this current study indicating an analytical reproducibility (mean difference) of
293 0.2‰ ($1\sigma = 0.5$, $n = 9$).
294
295 **Results**
296
297 OSL dating
298
299 The suitability of the quartz extracts for OSL dating was evaluated using a combined preheat
300 plateau and dose-recovery test. In ESM 3c, the result of this test is shown, indicating the given
301 dose of 70.2 Gy could be reproduced within a temperature range of 220°C to 260°C. In addition,
302 ESM 3a shows a typical OSL shine-down curve, displaying a bright OSL signal that is quickly
303 bleached to measurement background. Growth curves could be established with high precision,
304 with recycling ratios of 0.9-1.1 (ESM 3b). Thus, the OSL quartz behavior, the preheat plateau
305 and the dose-recovery tests demonstrate the suitability of the applied SAR protocol.
306 In Table 1, the analytical data for OSL age calculation, including the data for dose rate
307 determination are given. The results of the OSL age calculation ranging from 106.3 ± 7.4 to
308 88.5 ± 5.8 ka indicate the studied section can be assigned to MIS 5. The sample BT 1055 from
309 the lower part of the studied sediment unit (Fig. 2) has an OSL age of 103.4 ± 6.4 ka, the

310 following sample BT 1054 from the middle part of the 30-cm unit (Fig. 2) shows an age of
311 106.3 ± 7.4 ka, which is within errors still consistent with the stratigraphic order. Sample BT
312 1052 from the upper part (Fig. 2) reveals an age of 90.3 ± 9.2 ka. The sample BT 885, which
313 was previously taken in 2009, shows an age of 88.5 ±5.8 ka and correlates with the result of BT
314 1052 (Table 1).
315
316 Diatom assemblages and $\delta^{18}O_{diatom}$
317
318 The microscopic analyses of the samples reveal the sediments are rich in well-preserved diatom
319 valves (Fig. 3). In total, 50 species could be identified of which 44 species are benthic, that is
320 they prefer littoral rather than planktonic habitats (ESM 1, ESM 22). The number of species per
321 sample ranges from 19 to 30. Generally, most species are represented by a few valves only.
322 Benthic diatoms dominate the whole sequence (70 to 95%), especially in the uppermost
323 sediments, resulting in very low planktonic/benthic ratios (Fig. 4).
324 Using broken stick, only PCA axis 1 showed significant variation. PCA axis 1 sample
325 scores are therefore also plotted against depth in Fig. 4. These data show considerable variation,
326 superimposed on a strong directional change from the base of the sediment unit to about 25 cm,
327 before sample scores decline to the top of the profile. A moderate but significant Pearson
328 product moment correlation coefficient exists between PCA axis 1 sample scores and the P/B
329 ratio ($r = -0.618$; $p = 0.0001$). CONISS has delimited 3 zones (Kala-1 to Kala-3), with major
330 divisions at 13.75 cm and 23.25 cm (Fig. 4).
331 Kala-1: This zone is dominated by *Pseudostaurosira brevistriata* and *Rhopalodia*
332 *gibberula*, although the planktonic *Cyclotella meneghiniana* is also abundant, resulting in
333 highest P/B ratios for the sequence and lowest PCA axis 1 samples scores. *Halamphora*
334 *thermalis* is also relatively common. At this time, $\delta^{18}O_{diatom}$ values increase steadily to their
335 highest values of +34.2‰ at 11.5 cm.

336 Kala-2: This zone is delimited by a small peak in *P. brevistriata*, a P/B minimum and
337 declining $\delta^{18}O_{diatom}$ values. Within this zone, the most notable changes include declining *C.*
338 *meneghiniana* values and increases in *Epithemia sorex*.
339 Kala-3: This zone is delimited by very low P/B ratio values and high PCA axis 1
340 samples, and lowest $\delta^{18}O_{diatom}$ values (+28.2‰ at 23.5 cm). During this zone, *C. meneghiniana*
341 values are generally at their lowest, while *E. sorex* values are at their highest. Towards the top
342 of this zone, P/B ratio values increase slighty, concomitant with declining PCA axis 1 sample
343 scores and increasing $\delta^{18}O_{diatom}$ values to about +31‰.
344 The inferred hydrological parameters (salinity, trophic status, pH) show little variation
345 throughout the palaeolake-phase. Most diatoms are tolerant to salinity fluctuations but about
346 15% of the species of the assemblages reflect oligohaline conditions in zones Kala-1 and -2
347 with an increase to 20% in Kala-3. About 60% of the diatom species indicate eutrophic
348 conditions and 20-30% are nutrient-tolerant. The pH reconstruction indicates alkaline
349 conditions (> 7). Approximately 30-40% of the diatom species require pH values of 7-8 and
350 50-80% of 8-9 with slight decrease of alkalinity during zone Kala-3.
351
352 **Discussion**
353
354 Dating
355
356 Age calculation of mega-lake phases in the MOZB (Fig. 1) have previously been established
357 using a large set of OSL dates from palaeo-shoreline features (Burrough and Thomas 2009;
358 Burrough et al. 2009a, 2009b). In respect of MIS 5, Burrough et al. (2009a) identified two
359 highstands of Lake Palaeo-Makgadikgadi centred at *c.* 105 ka and *c.* 92 ka respectively,
360 analysed as "events of unknown duration" (Burrough et al. 2009b). In contrast to samples
361 obtained from shoreline sediments (Burrough et al. 2009a), which may have been reworked by

362 waves, we dated quartz grains from a low energy aquatic milieu. The fine lamination of the
363 sediments indicates still water conditions below the wave-line and reworking of the sediments
364 can likely be ruled out. The range of our dates, however, shows large uncertainty remains.
365 Considering the uncertainties of the oldest (106.3 ± 7.4 ka) and the youngest age (88.5 ± 5.8
366 ka), the max. range is 113.7-82.7 ka, a period of 31 ka covering roughly MIS 5d-b, and the min.
367 range is 98.9-94.3 ka, a period of 4.6 ka.

368 The range has to be considered in the context of the duration of continuous deposition
369 of 30 cm of lacustrine sediments. In comparision with lake systems showing at least partly
370 similar (palaeo-)environmental settings (Aral Sea: 30 cm ~650 years, Filippov and Riedel 2009;
371 Lake Titicaca: 30 cm ~900-1200 years, Fornace et al. 2014; Tso Moriri, Ladakh, India: 30 cm
372 ~1100 years, Leipe et al. 2014; Lake Kotokel, Buryatia, Russia: 30 cm ~700 years, Kostrova et
373 al. 2016; Lake Teletskoye, Russian Altai: 30 cm ~600 years, Mitrofanova et al. 2016; Lake
374 Van, Turkey: 30 cm ~1000 years, North et al. unpublished data) it can be roughly estimated
375 that the 30-cm sediment unit of the Boteti section had been deposited during a period of
376 approximately 1 ka.

377 It is possible, but not likely that the terminal highstand is not archived in the 30-cm unit.
378 This could be because of potential deflation processes after the lake level had decreased. Once
379 exposed, sediments of such composition usually harden quickly under a (semi-)arid climate and
380 subsequent weathering and erosion processes are limited. This is also due to the fact that under
381 retreating lake levels, aeolian activity is increasing and consolidated lacustrine sediment
382 sequences are often, instead of being deflated, covered by sand (as can be observed across the
383 MOZB), which protects them from erosion. Moreover, the 40-cm-lacustrine-sediment unit at
384 the base of the Boteti section, which is overlain by playa sediments, appears to be complete and
385 provides an independant example of a relatively short lake highstand. We thus can provide at
386 least a first idea how long so-called mega-lake phases may have lasted.

387 The estimation that the 30-cm-sediment unit covers a period of not more than
388 approximately 1 ka allows us to infer a temporal resolution of the analysed samples of 1-2
389 decades. Dating uncertainties remains a major challenge for an accurate reconstruction of
390 environmental dynamics in the Kalahari, and is probably responsible for most of the
391 controversial discussions related to (Street and Grove 1976; Heine 1981, 1987, 1988; Stokes et
392 al. 1997; Gasse et al. 2008; Burrough and Thomas 2009; Burrough et al. 2009a, 2009b; Chase
393 and Brewer 2009; Hürkamp et al. 2011; Riedel et al. 2014; Burrough 2016).

394 Significant uncertainties also exist with respect to measured palaeo-shoreline altitudes.
395 In a number of studies the uncertainty is as high or even higher as the 9 m difference between
396 the 936 and 945 m a.s.l. palaeo-shorelines (Riedel et al. 2014). On the other hand, it is unlikely
397 mega-lake highstands reached the same elevation repeatedly, except in exceptional
398 circumstances. The two different lacustrine sediment units of the Boteti section indicate two
399 lake periods at the same position, which means they are of likely similar extension, although
400 the older highstand is about 9.3 m lower than the younger one. The amount of available water
401 during these two periods may have been similar, pointing at comparable climate settings, but
402 with increased accumulation of sediments in the MOZB raising the lake floor (Haddon and
403 McCarthy 2005). Thus a higher lake level of significant younger age than an earlier lower lake
404 level could have potentially been reached even with less hydrological input.

405

406 Diatom assemblages and $\delta^{18}O_{diatom}$

407

408 The diatom assemblage presented here is very different from contemporary flora found in the
409 fresh, shallow waters of the Okavango Delta (Mackay et al. 2012). The dominance of benthic
410 taxa (Fig. 4) in the BT unit indicates the persistence of shallow water conditions and extensive
411 littoral regions, especially during the terminal stages of sediment accumulation (zone Kala-3).
412 Patrick (1977) described *E. sorex* as an aerophilous species that can persist in environments

413 characterized by desiccation. Therefore, an increase of the abundance of *E. sorex* within the
414 sediments at this time potentially shows a stronger proximity to the shoreline caused by a drop
415 in lake level during this period of inferred lake level decline. The maximum water depth can be
416 calculated in the hydromorphological context to have been a few metres only (max. depth of
417 palaeolake ~50 m). The diatom assemblages reveal changes in lake water depth throughout the
418 record. The significant correlation between PCA axis 1 sample scores and P/B ratio suggests
419 varying water levels influenced diatom composition in the shallow lake waters. What is notable
420 is the period of highest P/B ratio is coincident with increasing $\delta^{18}O_{diatom}$ values (increasing
421 effective moisture), indicative of increasing planktonic habitats in this part of the lake (Fig. 4).
422 These shallow waters were likely freshwater to brackish; qualitative salinity
423 reconstruction indicate oligohaline conditions (0.5 to < 5 psu) persisted during the whole period
424 (Fig. 4). For example, the dominant species *P. brevistriata, R. gibberula* and *M. elliptica* have
425 wide salinity tolerances (Caljon and Cocquyt 1992; Krammer and Lange-Bertalot 1999; van
426 Dam et al. 1994; Stachura-Suchoples 2001). *E. sorex* is also described from oligohaline waters
427 (Cholnoky 1968; Patrick 1977; Krammer and Lange-Bertalot 1999; Kelly et al. 2005), while *C.*
428 *meneghiniana* is often found in brackish water (Hecky and Kilham 1973).
429 The qualitative oligohaline salinity reconstruction at the study site does not mean that
430 Lake Palaeo-Makgadikgadi was oligohaline in general but exhibited salinity gradients. Filling
431 up and interconnecting the lacustrine basins to a single lake (Fig. 1) required significant inflow
432 from at least one of the major river systems, either from the Okavango River in the (north-)west
433 or from the Okwa River in the southwest. It also cannot be ruled out that both river systems
434 were active simultaneously. If the Okavango was the main source of hydrological input, the
435 main lacustrine depression of the palaeolake-system, the Makgadikgadi Basin, would have
436 acted as a terminal lake with increasing salinity to the east (Fig. 1). The likely outflow in this
437 scenario would be through the Zambezi valley. Therefore, western lake areas between major
438 inflow and outflow would have been under freshwater conditions. An example of a comparator

439 to this behaviour can be found at extant Bosten Lake, Xinjiang, China, where inflow and
440 outflow are located at the western side of the lake and freshwater conditions prevail only there,
441 while the largest part of the water body is oligohaline (Mischke and Wünnemann 2006; Wufuer
442 et al. 2014; personal observation FR). A second scenario considers the Okwa River the main
443 source of water inflow during the highstand. In this case the Makgadikgadi Basin was exorheic
444 and the study site would have been in proximity to the outflow. In both scenarios freshwater
445 areas are limited, and considering the relatively short period of approximately 1 ka, the mega-
446 lake phase likely did not foster evolutionary radiations of freshwater fish or gastropods. This is
447 in agreement with the phylogeographic studies of Joyce et al. (2005) and Schultheiß et al.
448 (2014) who considered Early to Middle Pleistocene age of Lake Palaeo-Makgadikgadi
449 evolutionary radiations, indicating palaeohydrology and hydromorphology differed
450 significantly from our observed MIS 5 setting.

451 In respect of pH, it can be inferred from the diatoms that the lake was always alkaline
452 (pH ~8). Whereas *C. meneghiniana*, *E. sorex*, *H. thermalis* and *R. gibberula* occur preferentially
453 in waters with the pH greater than 8 (Cholnoky 1968; Gasse 1986; Gasse et al. 1995; van Dam
454 et al. 1994), *M. elliptica* and *P. brevistriata* predominantly occur in circumneutral to low
455 alkaline waters (pH = 7-8; Cholnoky 1968; Gasse 1986; van Dam et al. 1994; Stachura-
456 Suchoples 2001; Fig. 4). In addition, *P. brevistriata*, *C. meneghiniana*, and *E. sorex* indicate
457 elevated trophic levels troughout the record (Cholnoky 1968; van Dam et al. 1994; Gasse et al.
458 1995; Krammer and Lange-Bertalot 2000; Stachura-Suchoples 2001; Kelly et al. 2005).

459 The $\delta^{18}O_{diatom}$ data reflects the oxygen isotope composition of lake water ($\delta^{18}O_{lake}$), and
460 the water temperature at the time of frustule formation (Leng and Barker 2006; Leng and
461 Henderson 2013). In turn, $\delta^{18}O_{lake}$ is controlled by the isotopic composition of precipitation
462 ($\delta^{18}O_p$) re-charging the lake and the balance of evaporation over precipitation on the lake. Open
463 lake systems that have permanent river inflow and outflow have short residence times, and as
464 a result $\delta^{18}O_{diatom}$ tends to reflect changes in $\delta^{18}O_p$. Whereas in closed lakes that have no

465 discernable outflow, $\delta^{18}O_{lake}$ is usually influenced by evaporation of surface waters, and as a
466 result $\delta^{18}O_{diatom}$ reflects the moisture balance (precipitation over evaporation) of the region
467 (Leng and Marshall 2004; Leng and Barker 2006; Leng and Henderson 2013).

468 There is scant information about the isotope composition of precipitation ($\delta^{18}O_p$) in
469 Botswana, and southern Africa in general, with much of our understanding of isotope dynamics
470 linked to changes in Late Pleistocene groundwater and speleothem $\delta^{18}O$ records (de Vries et al.
471 2000; Lee-Thorp et al. 2001; Holmgren et al. 2003; Kulongoski and Hilton 2004). The ^{18}O
472 enrichment of older groundwaters in Uitenhage, South Africa, have previously been interpreted
473 in terms of a change in moisture source, with a northeastward incursion of South Atlantic winter
474 precipitation, which displaces or mixes with monsoonal precipitation from the Indian Ocean in
475 south-western Africa (Stute and Talma 1998). By comparison, a more recent study from
476 Letlhakeng, southern Botswana, suggests there was no role for Atlantic-sourced moisture and
477 that the Indian Ocean has been the dominant moisture source over the southern Kalahari since
478 the Late Pleistocene through to the present day (Kulongoski and Hilton 2004). The influence
479 of the 'amount effect' on $\delta^{18}O_p$ has also been discounted, as modern $\delta^{18}O_p$ values for the region
480 range from 0 to –5‰, but the most depleted $\delta^{18}O_p$ values occur during months with the most
481 amount of rainfall (de Vries et al. 2000). As a result, Kulongoski et al. (2004) concluded that
482 Late Pleistocene groundwater $\delta^{18}O$ variability is caused by changes in atmosphere-$\delta^{18}O_p$
483 dynamics driven by changing sea surface temperatures.

484 A $\delta^{18}O$ speleothem record from Cold Air Cave in the Makapansgat Valley, northern South
485 Africa, was interpreted in terms of $\delta^{18}O_p$ variability caused by changes in the frequency of
486 intense convective storm events during the dry season that bring depeleted $\delta^{18}O_p$ (Rozanski et
487 al. 1993), against a background of persistent mid-latitude rain during the wet season (Holmgren
488 et al. 2003). As a result, higher or more positive $\delta^{18}O_p$ values reflect generally warmer, wetter
489 conditions while lower values suggest cooler, drier conditions. This interpretation is supported

490 by a 100-year data set from the region, which demonstrates a positive correlation between
491 measured regional temperatures and speleothem $\delta^{18}O$ (Lee-Thorp et al. 2001). In addition, an
492 observed correlation between regional temperature and precipitation and speleothem colour,
493 layer thickness and $\delta^{18}O$ further supports the interpretation that lighter $\delta^{18}O_p$ is representative
494 of drier, colder conditions over southern Africa (Holmgren et al. 1999).

495 The $\delta^{18}O_{diatom}$ record from the BT unit spans approximately 1 ka sometime during MIS 5d-
496 b and shows decadal to bi-decadal variability. Based on the interpretative framework for
497 changes in $\delta^{18}O_p$ during the Late Pleistocene set out above, the shift in $\delta^{18}O_{diatom}$ from +30.5‰
498 at the base of the sediment unit to higher values of +34.2‰ at 11.5 cm would indicate
499 increasingly warmer and wetter conditions during this period (Fig. 4). The lower $\delta^{18}O_{diatom}$
500 values would be driven by the enhancement of a wet season over the Kalahari and an subsequent
501 increase in lake level. This observation is consistent with the increase in P/B ratio (Fig. 4),
502 suggesting an increase in planktonic habitats associated with greater lake levels. Moreover, on
503 top of an increasing lake level, the lake water would also be undergoing enhanced evaporation
504 because of the generally warmer conditions, and therefore lake waters would also become
505 further enriched in ^{18}O. Taken together, the shift to a dominant wet season and greater
506 evaporation would both drive $\delta^{18}O_{diatom}$ to the more positive values observed in our record (Fig.
507 4). However, it is difficult to tease out which would be the dominant mechansism, and the
508 $\delta^{18}O_{diatom}$ record is likely to reflect a combination of both.

509 After the initial increase there are a number of significant fluctuations in $\delta^{18}O_{diatom}$ from
510 ~+34 to +30.5‰ between 11.5 – 19.5 cm (Fig. 4), which broadly mirror changes in P/B, and
511 could reflect variability between warm-wet and cold-arid climate, as well as the subsequent
512 changes in evaporative concentration of Lake Palaeo-Makgadikgadi. Following this, the shift
513 to the lowest $\delta^{18}O_{diatom}$ values in our record occurs at 23.5 cm (Fig. 4), which we interpret as a
514 shift to colder and more arid conditions, as well as a lowering of lake level as indicated by the

515 P/B ratio from the diatom assemblages. The return to more positive $\delta^{18}O_{diatom}$ values after this
516 event (Fig. 4) could reflect a shift back to a warm, wet environment, but as the P/B ratios show,
517 lake levels remain low and so could reflect enhanced evaporation of lake water during this arid
518 stage in climate.

519 The relatively short duration of the mega-lake phase of approximately 1 ka under a
520 generally arid climate over large parts of southern Africa during MIS 5 (Scholz et al. 2007;
521 Urrego et al. 2015) suggests we may have captured a climate event at the scale of a Heinrich
522 event (Bond and Lotti 1995, Broecker 2002). Previous studies have modelled the impact of
523 Heinrich events on South Atlantic sea surface temperatures, which increase abruptly ("Atlantic
524 Heat Piracy Model", Ganopolski and Rahmstorf 2001; Seidov and Maslin 2001). The climatic
525 effect of northern hemisphere triggered Heinrich events on the southern hemisphere has also
526 been identified in Antarctica ice cores (Jouzel et al. 2007). The observation of Urrego et al.
527 (2015) that during climate transitions between warm and cold or cold and warm, humidity
528 during arid MIS 5 temporarily increased, supports the idea of a Heinrich event-like climate
529 period. Our record thus demonstrates the decadal to bi-decadal climate variability during such
530 an event.

531 Our data cannot contribute to the discussion whether the MIS 5 climate extremes
532 triggered large scale early human migration across and ultimatively out of Africa (Carto et al.
533 2009; Rito et al. 2013). The data, however, can contribute to the discussion why the Kalahari
534 hunter-gatherers, i.e. the Khoisan-speaking Bushmen groups, represent the genetically most
535 divergent population in the world (Tishkoff et al. 2007; Li et al. 2008; Henn et al. 2011). High
536 genetic variation means high adaptation potential (Charlesworth 2009). Semi-arid areas such as
537 the Kalahari are particularly vulnerable because small negative changes in precipitation amount
538 or in rainfall seasonality may trigger major changes in the environment and thus largely control
539 the habitability. Even under the assumption of large dating uncertainties, it is clear that
540 anatomically modern humans have lived in the Kalahari during MIS 5 and the climate extremes

541 likely triggered migration to environmentally more favourable regions. On the other hand it is
542 evident that Khoisan-speaking groups have adapted to arid climate, exhibiting traits which are
543 absent in other human groups such as the ability to store water and lipid metabolites in body
544 tissues (Schuster et al. 2010). Considering these adaptations in the context of archaeological
545 findings (Robbins et al. 2016), it can be assumed that Khoisan-speaking groups have lived
546 permanently in (semi-)arid environments since MIS 5, that is they probably never left the
547 Kalahari as other human groups did. The environmental history of the Kalahari since MIS 5
548 appears to be that of a highly dynamic and thus often fragmented ecosystem; habitat
549 fragmentation leading to human population fragmentation. Small populations however are
550 prone to genetic drift, which results in loss of genetic variation (Charlesworth 2009). Against
551 this background it can be suggested that the Khoisan-speaking groups have not been fragmented
552 into small populations but represented a relatively large human population all over the Kalahari.
553 This was possible only if these humans and the animals they hunted had access to potable water.
554 The here studied MIS 5 lake highstand in the MOZB of approximately 1 ka appears to
555 be a relatively short period, which however, can be compared with the tip of an iceberg. We do
556 not know how far the lake regressed after the highstand. We do not know how the seasonality
557 of MIS 5 rainfall was. We do not know which rivers were active during which period of
558 supposedly extra-arid MIS 5, except that we can assume from the geographical settings of
559 headwaters that Okavango, Orange and Zambezi rivers were likely perennial even during
560 megadroughts. These river systems however cannot have been the only sources of potable water
561 because otherwise the Khoisan-speaking population would have been fragmented, which
562 evidently was not the case. The idea that the Kalahari was even drier than present-day during
563 much of the last approximately 100 ka as was postulated for MIS 5 (Urrego et al. 2015) or for
564 the Last Glacial Maximum (LGM; Riedel et al. 2014) must be questioned. Gasse et al. (2008)
565 saw evidence for enhanced humidity over parts of south-western Africa during LGM. Hürkamp
566 et al. (2011) proposed winter rainfall in addition to summer rainfall over the southern Kalahari

567 during this period and Riedel et al. (2014) suggested that the Okwa River (Fig. 1) was fully
568 active during the LGM. It thus can be speculated that future studies of MIS 5 climate over the
569 Kalahari may exhibit the environment was more favourable for humans than supposed.
570
571 **Conclusions**
572
573 OSL ages suggest the identified mega-lake phase in the Kalahari occurred during a period of
574 MIS 5d-b. The climate over southern Africa during MIS 5 was considered to have been
575 (extremely) arid (Scholz et al. 2007; Urrego et al. 2015), although Urrego et al. (2015) identified
576 short excursions to more humid conditions during cold-warm and warm-cold transitions. One
577 of these humid periods triggered a highstand at Lake Palaeo-Makgadikgadi of about 935-940
578 m a.s.l. for approximately 1 ka, as is tentatively estimated here based on the potential
579 sedimentation rate of the studied section. This short-term hydrologically favorable phase is at
580 the scale of a North Atlantic-driven Heinrich event, and we speculate whether rapid increases
581 of southern Atlantic SSTs could have triggered significantly increased moisture supply over the
582 Kalahari and/or the Bié Plateau (Angola) where the (nowadays) active catchment of the
583 Okavango river system is located (Fig. 1).
584 The studied section is in close proximity to the palaeo-shore of the mega-lake and based
585 on the P/B ratio of diatom assemblages we infer shallow water conditions prevailed at the site.
586 The analysed diatom assemblages indicate an alkaline and oligohaline lake, although the
587 reconstructed salinity is not representative of the whole mega-lake because the studied section
588 is located about 100-150 km away from the two major inflow systems, the Okavango River in
589 the (north-)west and the Okwa River in the southwest of the lacustrine basins (Fig. 1). As we
590 could not infer which of the inflow systems was active during the highstand, a salinity gradient
591 from freshwater to oligohaline either existed off the Okavango or Okwa river mouths.

592 Considering the role Pleistocene Lake Palaeo-Makgadikgadi is likely to have played in
593 the phylogeography of freshwater fish (Joyce et al. 2005) or freshwater gastropods (Schultheiß
594 et al. 2014), we suggest the mega-lake phase in this study is too short a duration that is
595 dominated by oligohaline conditions, and therefore it was not a suitable trigger for evolutionary
596 radiations of freshwater taxa. The comparatively high temporal resolution of 1-2 decades of our
597 studied samples provides valuable insights of climate variability during a mega-lake phase.
598 Albeit significant changes in $\delta^{18}O_{diatom}$ values occurred (Fig. 4), the highstand is considered a
599 hydrologically stable period.
600 Although the studied mega-lake period was likely a short-term climate anomaly possibly
601 triggered by North-Atlantic iceberg discharges, it is challenging the view that MIS 5 was mostly
602 extremely dry. That the environment may have hydrologically been more favourable, is
603 supported by archaeological and genetic data suggesting permanent human occupation of the
604 Kalahari since MIS 5.
605
606 **Acknowledgements**
607
608 We appreciate the field assistance of Franziska Slotta (FU Berlin, Germany), Linda Taft
609 (University of Bonn, Germany), Michael Taft (Abenden, Germany), Karl-Uwe Heußner and
610 Alexander Janus (both German Archaelogical Institute, Berlin). Maike Glos (FU Berlin) helped
611 processing samples and Jan Evers (FU Berlin) designed Figure 1 and helped improving further
612 figures. Many thanks to Manfred Fischer (University of Bayreuth, Germany) for dose rate
613 determination. We also like to thank the reviewers for constructive criticism. The Ministry of
614 Minerals, Energy and Water Resources of Botswana kindly granted a research permit. FR is
615 grateful to the Deutsche Forschungsgemeinschaft for financial support.
616
617 **References**

618

619 Balter M (2002) What made humans modern? Science 295(5558):1219-1225

620 Batisani N, Yarnal B (2010) Rainfall variability and trends in semi-arid Botswana: Implications
621 for climate change adaptation policy. Appl Geogr 30:483-489

622 Battarbee RW, Carvalho L, Jones VJ, Flower RJ, Cameron NG, Bennion H, Juggins S (2001)
623 Diatoms. In: Smol JP, Birks HJB, Last WM (eds) Tracking environmental change using
624 lake sediments, vol 3. Kluwer Academic Publishers, Dordrecht, pp 155-202

625 Bond GC, Lotti R (1995) Iceberg discharges into the North Atlantic on millennial time scales
626 during the last glaciation. Science 267:1005-1017

627 Bøtter-Jensen L (1997) Luminescence techniques: Instrumentation and methods. Radiat Meas
628 17:749-768

629 Broecker WS (2002) Massive iceberg discharges as triggers for global climate change. Nature
630 372:421-424

631 Burrough SL (2016) Late Quaternary environmental change and human occupation of the
632 southern African interior. In: Jones SC, Stewart BA (eds) Africa from MIS 6-2: Population
633 dynamics and palaeoenvironments – Vertebrate Paleobiology and Paleoanthropology
634 Series. Springer, Heidelberg, pp 161-174

635 Burrough SL, Thomas DSG (2009) Geomorphological contributions to palaeolimnology on the
636 African continent. Geomorphology 103:285-298

637 Burrough SL, Thomas DSG, Bailey RM (2009a) Mega-lake in the Kalahari: a late Pleistocene
638 record of the Palaeolake Makgadikgadi system. Quat Sci Rev 28:1392-1411

639 Burrough SL, Thomas DSG, Singarayer JS (2009b) Late Quaternary hydrological dynamics in
640 the Middle Kalahari: forcing and feedbacks. Earth-Sci Rev 96:313-326

641 Caljon AG, Cocquyt CZ (1992) Diatoms from surface sediments of the northern part of Lake
642 Tanganyika. Hydrobiologia 230:135-156

643 Carto SL, Weaver AJ, Hetherington R, Lam Y, Wiebe EC (2009) Out of Africa and into an ice
644 age: on the role of global climate change in the late Pleistocene migration of early modern
645 humans out of Africa. J Hum Evol 56:139-151
646 Chapligin B, Leng MJ, Webb E, Alexandre A, Dodd JP, Ijiri A, Lücke A, Shemesh A,
647 Abelmann A, Herzschuh H, Longstaffe FJ, Meyer H, Moschen R, Okazaki Y, Rees NH,
648 Sharp ZD, Sloane HJ, Sonzongi C, Swann JEA, Sylvestre F, Tyler JJ, Yam R (2011) Inter-
649 laboratory comparison of oxygen isotope compositions from biogenic silica. Geochim
650 Cosmochim Acta 75:7242-7256
651 Charlesworth B (2009) Effective population size and patterns of molecular evolution and
652 variation. Nat.Rev Genet 10:195-205
653 Chase BM, Brewer S (2009) Last Glacial Maximum dune activity in the Kalahari desert of
654 southern Africa: observations and simulations. Quat Sci Rev 28:301-307
655 Chase BM, Meadows ME (2007) Late Quaternary dynamics of southern Africa´s winter rainfall
656 zone. Earth-Sci Rev 84:103-138
657 Chase BM, Scott L, Meadows ME, Gil-Romera G, Boom A, Carr AS, Reimer PJ, Truc L,
658 Valsecchi V, Quick LJ (2012) Rock hyrax middens: a palaeoenvironmental archive for
659 southern African drylands. Quat Sci Rev 56:107-125
660 Cholnoky BJ (1968) Die Ökologie der Diatomeen in Binnengewässern (Ecology of diatoms in
661 inland waters). Cramer J, Lehre, Germany
662 Cohen AS, Stone JR, Beuning KRM, Park LE, Reinthal PN, Dettman D, Scholz CA, Johnson
663 TC, King JW, Talbot MR, Brown ET, Ivory SJ (2007) Ecological consequences of early
664 Late Pleistocene megadroughts in tropical Africa. PNAS 104(42):16422-16427
665 Cooke HJ (1979) The origin of the Makgadikgadi Pans. Botsw Notes Rec 11:37-42
666 Cooke HJ (1980) Landform evolution in the context of climatic change and neo-tectonism in
667 the Middle Kalahari of north-central Botswana. Trans Inst Br Geogr 5:80-99

668 Cooke HJ, Verstappen HT (1984) The landforms of the western Makgadikgadi basin in northern
669 Botswana, with consideration of the chronology of the evolution of Lake Palaeo-
670 Makgadikgadi. Z Geomorphol 28:1–19
671 Cordier S, Harmand D, Lauer T, Voinchet P, Bahain JJ, Frechen M (2012) Geochronological
672 reconstruction of the Pleistocene evolution of the Sarre valley (France and Germany) using
673 OSL and ESR dating techniques. Geomorphology 165-166:91-106
674 de Vries JJ, Selaolo ET, Beekman HE (2000) Groundwater recharge in the Kalahari, with
675 reference to paleo-hydrologic conditions. J Hydrol 238:110–123
676 Ebert JI, Hitchcock, RK (1978) Ancient lake Makgadikgadi, Botswana: mapping measurement
677 and palaeoclimate significance. Palaeoecol Afr 10/11:47-56
678 Eckardt FD, Bryant RG, McCulloch G, Spiro B, Wood WW (2008) The hydrochemistry of a
679 semi-arid pan basin case study: Sua Pan, Makgadikgadi, Botswana. Appl Geochem
680 23:1563-1580
681 Filippov A, Riedel F (2009) The late Holocene mollusc fauna of the Aral Sea and its
682 biogeographical and ecological interpretation. Limnologica 39:67-85
683 Fornace KL, Hughen KA, Shanahan TM, Fritz SC, Baker PA, Sylvia SP (2014) A 60,000-year
684 record of hydrologic variability in the Central Andes from the hydrogen isotopic
685 composition of leaf waxes in Lake Titicaca sediments. Earth Planet Sci Lett 408:263-271
686 Gabriel KR (2002) Goodness of fit of biplots and correspondence analysis. Biometrika 89:423-
687 436
688 Ganopolski A, Rahmstorf S (2001) Rapid changes of glacial climate simulated in a coupled
689 climate model. Nature 409:153-158
690 Gasse F (1986) East African diatoms – Taxonomy, ecological distribution. Bibl Diatomol 11:1–
691 201

692 Gasse F, Juggins S, Ben Khelifa L (1995) Diatom-based transfer functions for inferring past
693 hydrochemical characteristics of African lakes. Palaeogeogr, Palaeoclimatol, Palaeoecol
694 117:31-54
695 Gasse F, Chalié F, Vincens A, Williams MAJ, Williamson D (2008) Climatic patterns in
696 equatorial and southern Africa from 30,000 to 10,000 years ago reconstructed from
697 terrestrial and near-shore proxy data. Quat Sci Rev 27:2316-2340
698 Genner MJ, Seehausen O, Lunt DH, Joyce DA, Shaw PW, Carvalho GR, Turner GF (2007)
699 Age of cichlids – new dates for ancient fish radiations. Mol Biol Evol 24:1269-1282
700 Geyh MA, Heine K (2014) Several distinct wet periods since 420 ka in the Namib Desert
701 inferred from U-series dates of speleothems. Quat Res 81(2):381-391
702 Grey DRC, Cooke HJ (1977) Some problems in the Quaternary evolution of the landforms of
703 northern Botswana. Catena 4:123-133
704 Grimm EC (1991-2011) Tilia®Version 1.7.16 [Computer Software] Illinois State Museum,
705 Research and Collection Center, Springfield
706 Grove AT (1969) Landforms and climatic change in the Kalahari and Ngamiland. Geogr J
707 135:191-212
708 Gumbricht T, McCarthy TS, Merry CL (2001) The topography of the Okavango Delta,
709 Botswana, and its tectonic and sedimentological implications. S Afr J Sci 104:243-264
710 Haddon IG, McCarthy TS (2005) The Mesozoic-Cenozoic interior sag basins of central Africa
711 – The Late-Cretaceous-Cenozoic Kalahari and Okavango basins. J Afr Earth Sci 43:316-
712 333
713 Hecky RE, Kilham P (1973) Diatoms in alkaline, saline lakes: Ecology and geochemical
714 implications. Limnol Oceanogr 18:53-71
715 Heine K (1981) Aride und pluviale Bedingungen während der letzten Kaltzeit in der Südwest-
716 Kalahari (südliches Afrika)(Arid and pluvial conditions during the last glacial in the
717 southwest Kalahari (southern Africa)). Z Geomorphol NF, Suppl 38:1-37

718 Heine K (1982) The main stages of the Late Quaternary evolution of the Kalahari region,
719 southern Africa. Palaeoecol Afr 15:53-76
720 Heine K (1987) Zum Alter jungquartärer Seespiegelschwankungen in der Mittleren Kalahari,
721 südliches Afrika (On the age of late Quaternary lake level fluctuations in the Middle
722 Kalahari, southern Africa). Palaeoecol Afr 18:73-101
723 Heine K (1988) Southern African palaeoclimates 35-25 ka ago: a preliminary summary.
724 Palaeoecol Afr 19:305-315
725 Henn BM, Gignoux CR, Jobin M, Granka JM, Macpherson JM, Kidd JM, Rodríguez-Botigué
726 L, Ramachandran S, Hon L, Brisbin A, Lin AA, Underhill PA, Comas D, Kidd KK,
727 Norman PJ, Parham P, Bustamante CD, Mountain JL, Feldman MW (2011) Hunter-
728 gatherer genomic diversity suggests a southern African origin for modern humans. PNAS
729 108(13):5154-5162
730 Henshilwood CS, d'Errico F, Yates R, Jacobs Z, Tribolo C, Duller GAT, Mercier N, Sealy JC,
731 Valladas H, Watts I, Wintle AG (2002) Emergence of modern human behavior: Middle
732 Stone Age engravings from South Africa. Science 295(5558):1278-1280
733 Holmgren K, Lee-Thorp, JA, Cooper GRJ, Lundblad K, Partridge TC, Scott L, Sithaldeen R,
734 Talma AS, Tyson PD (2003) Persistent millennial-scale climatic variability over the past
735 25,000 years in Southern Africa. Quat Sci Rev 22:2311-2326
736 Holmgren K, Karlén W, Lauritzen SE, Lee-Thorp JA, Partridge TC, Piketh S, Repinski P,
737 Stevenson C, Svenered O, Tyson PD (1999) A 3000-year high-resolution stalagmite based
738 record of palaeoclimate for northeastern South Africa. Holocene 9:295-309
739 Hürkamp K, Völkel J, Heine K, Bens O, Leopold M, Winkelbauer J (2011) Late Quaternary
740 environmental changes from aeolian and fluvial geoarchives in the south-western Kalahari,
741 South Africa: implications for past African climate dynamics. S Afr J Geol 114:459-474
742 Ingman M, Kaessmann H, Pääbo S, Gyllensten U (2000) Mitochondrial genome variation and
743 the orgin of modern humans. Nature 408:708-713

744 Jacobs Z, Roberts RG (2009) Catalysts for Stone Age innovations. Commun Integr Biol
745 2(2):191-193
746 Jollifer IT (1986) Principal Components Analysis. Springer-Verlag, New York
747 Jouzel J, Masson-Delmotte V, Cattani O, Dreyfus G, Falourd S, Hoffmann G, Minster B, Nouet
748 J, Barnola JM, Chappellaz J, Fischer H, Gallet JC, Johnsen S, Leuenberger M, Loulergue
749 L, Luethi D, Oerter H, Parrenin F, Raisbeck G, Raynaud D, Schilt A, Schwander J, Selmo
750 E, Souchez R, Spahni R, Stauffer B, Steffensen JP, Stenni B, Stocker TF, Tison JL, Werner
751 M, Wolff W (2007) Orbital and millennial Antarctic climate variability over the past
752 800,000 Years. Science 317:793-796
753 Joyce DA, Lunt DH, Bills R, Turner GF, Katongo C, Duftner N, Sturmbauer C, Seehausen O
754 (2005) An extant cichlid fish radiation emerged in an extinct Pleistocene lake. Nature
755 435:90-95
756 Kelly MG, Bennion H, Cox EJ, Goldsmith B, Jamieson J, Juggins S, Mann DG, Telford RJ
757 (2005) Common freshwater diatoms of Britain and Ireland – an interactive key.
758 Environment Agency, Bristol: http://craticula.ncl.ac.uk/ EADiatomKey/html/taxa.html
759 Kinabo BD, Atekwana EA, Hogan JP, Modisi MP, Wheaton DD, Kampunzu AB (2007) Early
760 structural development of the Okavango rift zone, NW Botswana. J Afr Earth Sci 48:125-
761 136
762 Kostrova SS, Meyer H, Tarasov PE, Bezrukova EV, Chapligin B, Kossler A, Pavlova LA,
763 Kuzmin MI (2016) Oxygen isotope composition of diatoms from sediments of Lake
764 Kotokel. Russ Geol Geophys 57:1239-1247
765 Krammer K (2002) *Cymbella*. In: Lange-Bertalot H (ed) Diatoms of Europe, vol 3. ARG
766 Gantner Verlag KG, Ruggell
767 Krammer K, Lange-Bertalot H (1997) Bacillariophyceae. Part 1, Naviculaceae. In: Ettl H,
768 Gerloff J, Heynig H, Mollenhauer D (eds) Süßwasserflora von Mitteleuropa 2/1
769 (Freshwater flora from Central Europe). Spektrum Akademischer Verlag, Heidelberg

770 Krammer K, Lange-Bertalot H (1999) Bacillariophyceae. Part 2, Bacillariaceae,
771 Epithemiaceae, Surirellaceae. In: Ettl H, Gerloff J, Heynig H, Mollenhauer D (eds)
772 Süßwasserflora von Mitteleuropa 2/2 (Freshwater flora from Central Europe). Spektrum
773 Akademischer Verlag, Heidelberg, Berlin
774 Krammer K, Lange-Bertalot H (2000) Bacillariophyceae. Part 3, Centrales, Fragilariaceae,
775 Eunotiaceae. In: Ettl H, Gerloff J, Heynig H, Mollenhauer D (eds) Süßwasserflora von
776 Mitteleuropa 2/3 (Freshwater flora from Central Europe). Spektrum Akademischer Verlag,
777 Heidelberg, Berlin
778 Krammer K, Lange-Bertalot H (2004) Bacillariophyceae. Part 4, Achnanthaceae, Kritische
779 Ergänzungen zu *Achnanthes* s.i., *Navicula* s.str., *Gomphonema*. In: Ettl H, Gärtner G,
780 Heynig H, Mollenhauer D (eds) Süßwasserflora von Mitteleuropa 2/4 (Freshwater flora
781 from Central Europe). Spektrum Akademischer Verlag, Heidelberg, Berlin
782 Kulongoski JT, Hilton DR (2004) Climate variability in the Botswana Kalahari from the late
783 Pleistocene to the present day. Geophys Res Lett 31:doi:10.1029/2003GL019238
784 Kusber W-H, Cocquyt CZ (2012) *Craticula elkab* (O. Müller ex O. Müller) Lange-Bertalot,
785 Kusber & Cocquyt, comb. nov. - Typification and observations based on African sediment
786 core material. Diatom Res 22:117-126
787 Lee-Thorp JA, Holmgren K, Lauritzen SE, Linge H, Moberg A, Partridge TC, Stevenson C,
788 Tyson PD (2001) Rapid climate shifts in the southern African interior throughout the mid
789 to late Holocene. Geophys Res Lett 28:4507-4510
790 Leipe C, Demske D, Tarasov PE, Wünnemann B, Riedel F, HIMPAC project members (2014)
791 Potential of pollen and non-pollen palynomorph records from Tso Moriri (Trans-Himalaya,
792 NW India) for reconstructing Holocene limnology and human-environmental interactions.
793 Quat Int 348:113-129
794 Leng MJ, Barker PA (2006) A review of the oxygen isotope composition of lacustrine diatom
795 silica for palaeoclimate reconstruction. Earth-Sci Rev 75:5-27

796 Leng MJ, Henderson ACG (2013) Recent advances in isotopes as palaeolimnological proxies.
797 J Paleolimnol 49:481-496
798 Leng MJ, Marshall JD (2004) Palaeoclimate interpretation of stable isotope data from lake
799 sediment archives. Quat Sci Rev 23:811-831
800 Leng MJ, Sloane HJ (2008) Combined oxygen and silicon isotope analysis of biogenic silica. J
801 Quaternary Sci 23:313-319
802 Levkov Z (2009) *Amphora* sensu lato. In: Lange-Bertalot H (ed) Diatoms of Europe, vol 5,
803 ARG Gantner KG, Ruggell
804 Li JZ, Absher DM, Tang H, Southwick AM, Casto AM, Ramachandran S, Cann HM, Barsh
805 GS, Feldman M, Cavalli-Sforza LL, Myers RM (2008) Worldwide human relationships
806 inferred from genome-wide patterns of variation. Science 319(5866):1100-1104
807 Lotter AF, Birks HJB (1993) The impact of the Laacher See tephra on terrestrial and aquatic
808 ecosystems in the Black Forest, southern Germany. J Quaternary Sci 8:263-276
809 Mackay AW, Davidson T, Wolski P, Woodward S, Mazebedi R, Masamba WRL, Todd M
810 (2012) Diatom sensitivity to hydrological and nutrient variability in a subtropical, flood-
811 pulse wetland. Ecohydrology 5:491-502
812 Mallick DIJ, Habgood F, Skinner AC (1981) A geological interpretation of Landsat imagery
813 and airphotography of Botswana. Overseas Geol Mineral Resour 56:1-35
814 Marean CW, Bar-Matthews M, Bernatchez J, Fisher E, Goldberg P, Herries AIR, Jacobs Z,
815 Jerardino A, Karkanas P, Minichillo T, Nilssen PJ, Thompson E, Watts I, Williams HM
816 (2007) Early human use of marine resources and pigment in South Africa during the Middle
817 Pleistocene. Nature 449:905-909
818 Mischke S, Wünnemann B (2006) The Holocene salinity history of Bosten Lake (Xinjiang,
819 China) inferred from ostracod species assemblages and shell chemistry: Possible
820 palaeoclimatic implications. Quat Int 154-155:100-112
821 Mitrofanova EY, Sutchenkova OS, Lovtskaya OV (2016) Lake Teletskoye (Altai, Russia):

822 reconstruction of the environment and prediction for its changes according to the
823 composition and quantity of diatoms in the bottom sediments. Russ Geol Geophys
824 57:1321-1333
825 Moore AE, Cotterill FPD, Eckardt FD(2012) The evolution and ages of Makgadikgadi palaeo-
826 lakes – consilient evidence from Kalahari drainage evolution, Botswana. S Afr J Geol
827 115:385-413
828 Morley DW, Leng MJ, Mackay AW, Sloane HJ, Rioual P, Battarbee RW (2004) Cleaning of
829 lake sediments for diatom oxygen isotope analysis. J Paleolimnol 31:391-401
830 Murray A, Wintle A (2000) Luminescence dating of quartz using an improved single-aliquot
831 regenerative-dose protocol. Radiat Meas 32:57-73
832 Nugent C (1990) The Zambezi River – tectonism, climatic change and drainage evolution.
833 Palaeogeogr Palaeoclimat Palaeoecol 78:55-69
834 Passarge S (1904) Die Kalahari (The Kalahari). Dietrich Riemer, Berlin
835 Patrick R (1977) The ecology of freshwater diatoms – diatom communities. In: Werner D (ed)
836 The Biology of Diatoms. University of California Press, Berkeley, Los Angeles, pp 284-
837 332
838 Peel MC, Finlayson BL, McMahon TA (2007) Updated world map of the Köppen-Geiger
839 climate classification. HESSD 4:439-473
840 Podgorski JE, Green AG, Kgotlhang L, Kinzelbach WKH, Kalscheuer T, Auken E, Ngwisanyi
841 T (2013) Paleo-megalake and paleo-megafan in southern Africa. Geology 41:1155-1158
842 Prescott JR, Hutton JT (1994) Cosmic Ray Contributions to Dose Rates for Luminescence and
843 ESR Dating: Large Depths and Long-Term Time Variations. Radiat Meas 23:497-500
844 Riedel F, Erhardt S, Chauke C, Kossler A, Shemang E, Tarasov P (2012) Evidence for a
845 permanent lake in Sua Pan (Kalahari, Botswana) during the early centuries of the last
846 millenium indicated by distribution of Baobab trees (*Adansonia digitata*) on "Kubu Island".
847 Quat Int 253:67-73

848 Riedel F, Henderson ACG, Heußner KU, Kaufmann G, Kossler A, Leipe C, Shemang E, Taft
849 L (2014) Dynamics of a Kalahari long-lived mega-lake system – hydromorphological and
850 limnological changes in the Makgadikgadi Basin (Botswana) during the terminal 50 ka.
851 Hydrobiologia 739:25-53
852 Ringrose S, Huntsman-Mapila P, Kampunzu AB, Downey WS, Coetzee SH, Vink B, Matheson
853 W, Vanderpost C (2005) Sedimentological and geochemical evidence for palaeo-
854 environmental change in the Makgadikgadi subbasin, in relation to the MOZ rift
855 depression, Botswana. Palaeogeogr Palaeoclimatol Palaeoecol 217:265-287
856 Rito T, Richards MB, Fernandes V, Alshamali F, Cerny V, Pereira L, Soares P (2013) The first
857 modern human dispersal across Africa. PLOS ONE 8(11)e80031
858 Robbins LH, Brook GA, Murphy ML, Ivester AH, Campbell AC (2016) The Kalahari during
859 MIS 6-2 (190-12 ka): Archaeology, paleoenvironment, and population dynamics. In: Jones
860 SC, Stewart BA (eds) Africa from MIS 6-2: Population dynamics and palaeoenvironments
861 – Vertebrate Paleobiology and Paleoanthropology Series. Springer, Heidelberg, pp 175-
862 193
863 Rozanski K, Araguas-Araguas L, Gonfiantini R (1993) Isotopic patterns in modern global
864 precipitation. In: Climate change in continental isotopic records. Swart PK, Lohman KC,
865 McKenzie J, Savin S (eds), Geophysical Monograph 78:1-36
866 Schlungbaum G, Baudler H (2001) Die Vielfalt innerer Küstengewässer an der südlichen
867 Ostsee - eine Übersicht von der Flensburger Förde bis zum Kurischen Haff, Teil 1
868 Entwicklungsgeschichte, Morphologie, Hydrologie und Hydrographie (The diversity of
869 interior coastal waters at the southern Baltic Sea – an overview from the Flensburg Fjord
870 to the Curonian Lagoon, part 1 history of development, morphology, hydrology and
871 hydrography). Rostock Meeresbiolog Beitr 8:5-61
872 Scholz CA, Johnson TC, Cohen AS, King JW, Peck JA, Overpeck JT, Talbot MR, Brown ET,
873 Kalindekafe E, Amoako PYO, Lyons RP, Shanahan TM, Castañeda IS, Heil CW, Forman

874 SL, McHargue LR, Beuning KR, Gomez J, Pierson J (2007) East African megadroughts
875 between 135 and 75 thousand years ago and bearing on early-modern human origins. PNAS
876 104(42):16416-16421
877 Schultheiß R, Van Bocxlaer B, Riedel F, von Rintelen T, Albrecht C (2014) Disjunct
878 distributions of freshwater snails testify to a central role of the Congo system in shaping
879 biogeographical patterns in Africa. BMC Evol Biol 14:42
880 Schuster SC, Miller W, Ratan A, Tomsho LP, Giardine B, Kasson LR, Harris RS, Petersen DC,
881 Zhao FQ, Qi J, Alkan C, Kidd JM, Sun YZ, Drautz DI, Bouffard P, Muzny DM, Reid JG,
882 Nazareth LV, Wang QY, Burhans R, Riemer C, Wittekindt NE, Moorjani P, Tindall EA,
883 Danko CG, Siang Teo W, Buboltz AM, Zhang ZH, Ma QY, Oosthuysen A, Steenkamp
884 AW, Oosthuisen H, Venter P, Gajewski J, Zhang Y, Franklin Pugh B, Makova KD,
885 Nekrutenko A, Mardis ER, Patterson N, Pringle TH, Chiaromonte F, Mullikin JC, Eichler
886 EE, Hardison RC, Gibbs RA, Harkins TT, Hayes VM (2010) Complete Khoisan and Bantu
887 genomes from southern Africa. Nature 463:943-947
888 Seidov D, Maslin M (2001) Atlantic Ocean heat piracy and the bipolar climate see-saw during
889 Heinrich and Dansgaard-Oeschger events. J Quaternary Sci 16:321-328
890 Shaw PA, Stokes S, Thomas DSG, Davies FBM, Holmgren K (1997) Palaeoecology and age
891 of a Quaternary high lake level in the Makgadikgadi Basin of the Middle Kalahari,
892 Botswana. S Afr J Sci 93:273-276
893 Shemang EM, Molwalefhe LN (2011) Geomorphic landforms and tectonism along the eastern
894 margin of the Okavango Rift Zone, north western Botswana as deduced from geophysical
895 data in the area. In: Sharkov EV (ed) New frontiers in tectonic research – General problems,
896 sedimentary basins and island arcs. InTech, Rijeka, pp 169-182
897 Shi N, Schneider R, Beug HJ, Dupont LM (2001) Southeast trade wind variations during the
898 last 135 kyr: evidence from pollen spectra in eastern South Atlantic sediments. EPSL
899 187:311-321

900 Stachura-Suchoples K (2001) Bioindicative values of dominant diatom species from the Gulf
901 of Gdansk, Southern Baltic Sea, Poland. In: Jahn R, Kociolek JP, Witkowski A, Compère
902 P (eds) Lange-Bertalot Festschrift. ARG Gantner KG, Ruggell, pp 477-490
903 Stokes S, Thomas DSG, Washington R (1997) Multiple episodes of aridity in southern Africa
904 since the last interglacial period. Nature 388:154-158
905 Street FA, Grove AT (1976) Environmental and climatic implications of late Quaternary lake-
906 level fluctuations in Africa. Nature 261:385-390
907 Stute M, Talma AS (1998) Glacial temperature and moisture transport regimes reconstructed
908 from noble gases and $\delta^{18}O$, Stampriet aquifer, Namibia. In: Isotope techniques in the study
909 of environmental change. IAEA, Vienna, pp 307-318
910 Stuut JBW, Prins MA, Schneider RR, Weltje GJ, Jansen JHF, Postma G (2002) A 300-kyr
911 record of aridity and wind strength in southwestern Africa: inferences from grain-size
912 distributions of sediments on Walvis Ridge, SE Atlantic. Mar Geol 180:221-233
913 ter Braak CJF, Šmilauer P (2002) CANOCO Reference Manual and User's Guide to CANOCO
914 for Windows: Software for Canonical Community Ordination Version 4.5. Microcomputer
915 Power, Ithaca, New York
916 Thomas DSG, Shaw PA (1991) The Kalahari environment, Cambridge University Press,
917 Cambridge
918 Tishkoff SA, Gonder MK, Henn BM, Mortensen H, Knight A, Gignoux C, Fernandopulle N,
919 Lema G, Nyambo TB, Ramakrishnan U, Reed FA, Mountain JL (2007) History of click-
920 speaking populations of Africa inferred from mtDNA and Y chromosome genetic variation.
921 Mol Biol Evol 24(10):2180-2195
922 Urrego DH, Sánchez Goñi MF, Daniau AL, Lechevrel S, Hanquiez V (2015) Increased aridity
923 in southwestern Africa during the warmest periods of the last interglacial. Clim Past
924 11:1417-1431

925 van Dam H, Mertens A, Sinkeldam J (1994) A coded checklist and ecological indicator values
926 of freshwater diatoms from the Netherlands. Neth J Aquat Ecol 28:117–133
927 van Zinderen Bakker EM (1976) The evolution of Late-Quaternary palaeoclimates of southern
928 Africa. Palaeoecol Afr 9:160-202
929

Figure captions

Fig. 1. A. general location of study area. B. Map of Makgadikgadi-Okavango-Zambezi basin (MOZB) of the south-western branch of the East African Rift System and the major tributaries. Black dashed lines indicate valleys of palaeo-rivers. Major subbasins of MOZB shaded black. During late Quaternary hydrologically favourable periods these subbasins may have been part of a mega-lake. Due to tectonics and hydromorphological processes the modern setting can be used only tentatively for simulating past mega-lake sizes and shapes. C. A digital elevation model (modified from Riedel et al. 2014) exhibits the location of the studied geological section at the western edge of the Makgadikgadi Basin where palaeo-shorelines can be found on the structural Gidikwe Ridge.

Fig. 2. Upper part of the Boteti river valley section with studied 30-cm diatom-rich sediment unit on top (BT). Position of samples for OSL dating and OSL dates are indicated.

Fig. 3. Scanning electron microscope images of the six most abundant diatom species identified in the Boteti section top unit (BT). 1-2: *Cyclotella meneghiniana*, 3-4: *Pseudostaurosira brevistriata*, 5-6: *Mastogloia elliptica*, 7-8: *Rhopalodia gibberula*, 9-10: *Epithemia sorex*, 11-12: *Halamphora thermalis*.

Fig. 4. Composite diagram illustrating percentage abundances of most frequent species separated into benthic and planktonic forms, P/B ratio, log-centred PCA, $\delta^{18}O_{diatom}$ variability, and stack diagrams for salinity, trophy and pH inferred from the autecology of the diatom species.

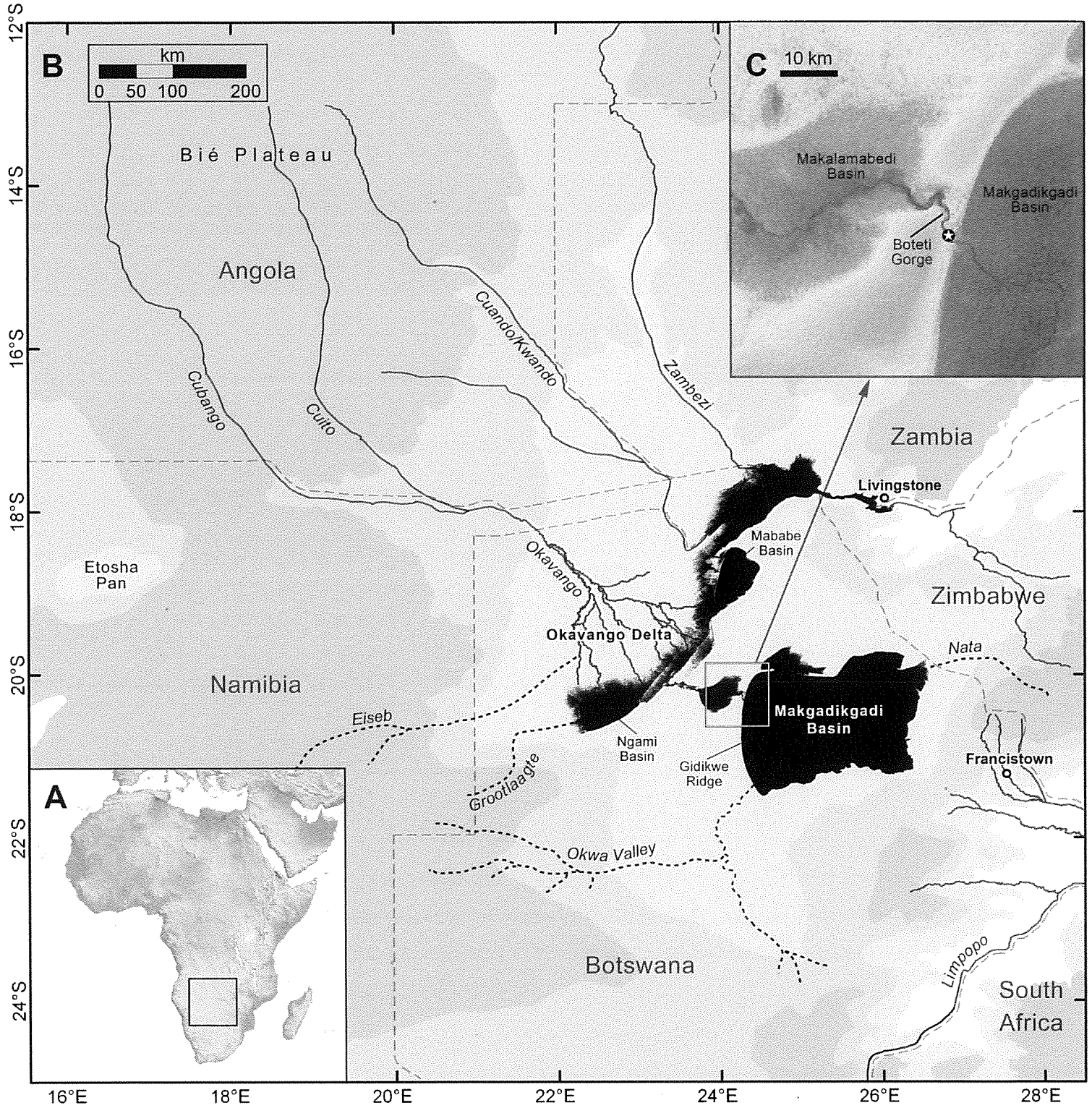
B
km
0 50 100 200
C
10 km
Bié Plateau
Angola
Cubango
Cuito
Cuando/Kwando
Zambezi
Zambia
Livingstone
Mababe Basin
Okavango
Okavango Delta
Etosha Pan
Namibia
Zimbabwe
Nata
Makgadikgadi Basin
Ngami Basin
Gidikwe Ridge
Francistown
Eiseb
Grootlaagte
Okwa Valley
Botswana
Limpopo
South Africa
Makalamabedi Basin
Makgadikgadi Basin
Boteti Gorge
A
12°S
14°S
16°S
18°S
20°S
22°S
24°S
16°E
18°E
20°E
22°E
24°E
26°E
28°E

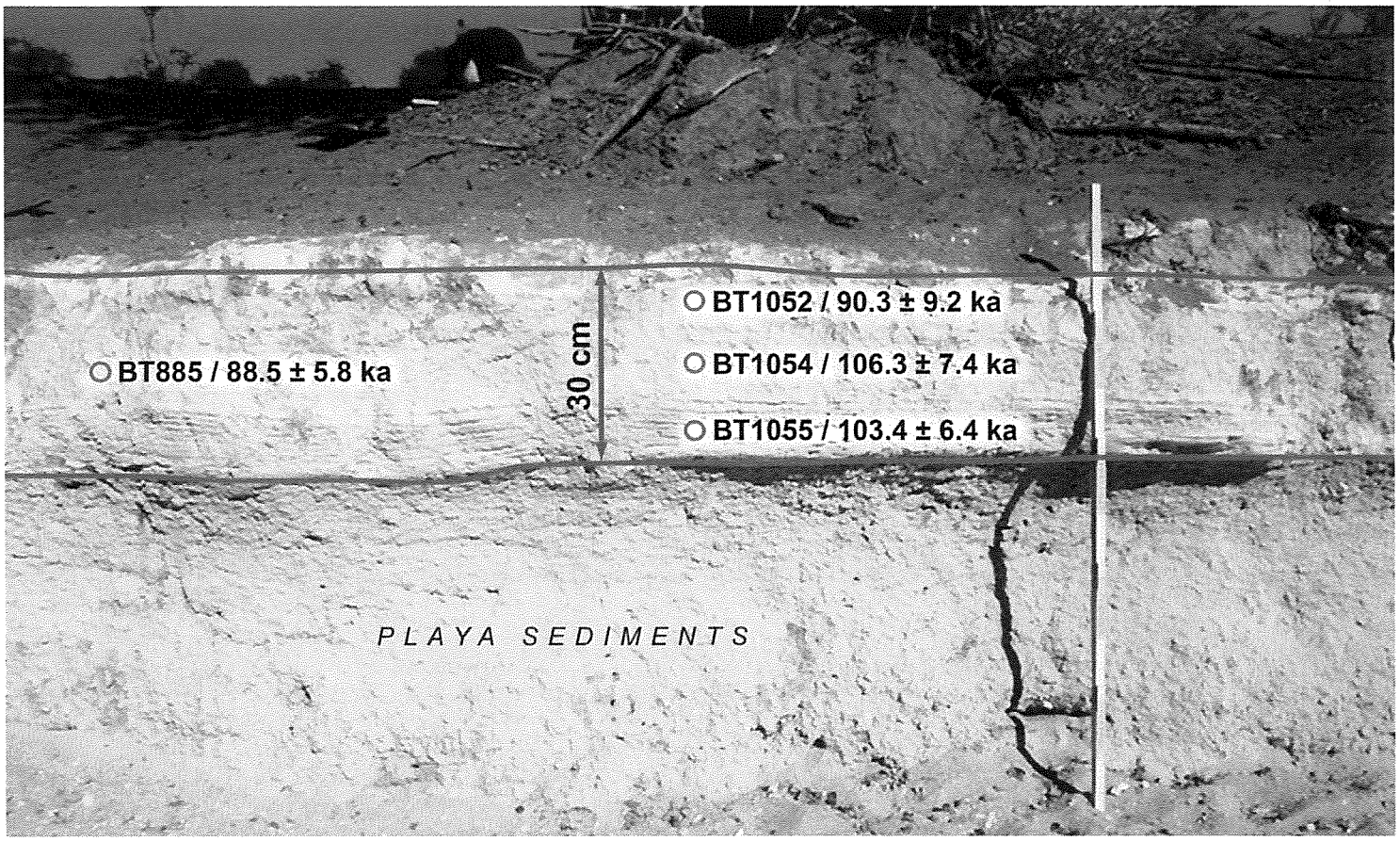
BT885 / 88.5 ± 5.8 ka
30 cm
BT1052 / 90.3 ± 9.2 ka
BT1054 / 106.3 ± 7.4 ka
BT1055 / 103.4 ± 6.4 ka
PLAYA SEDIMENTS

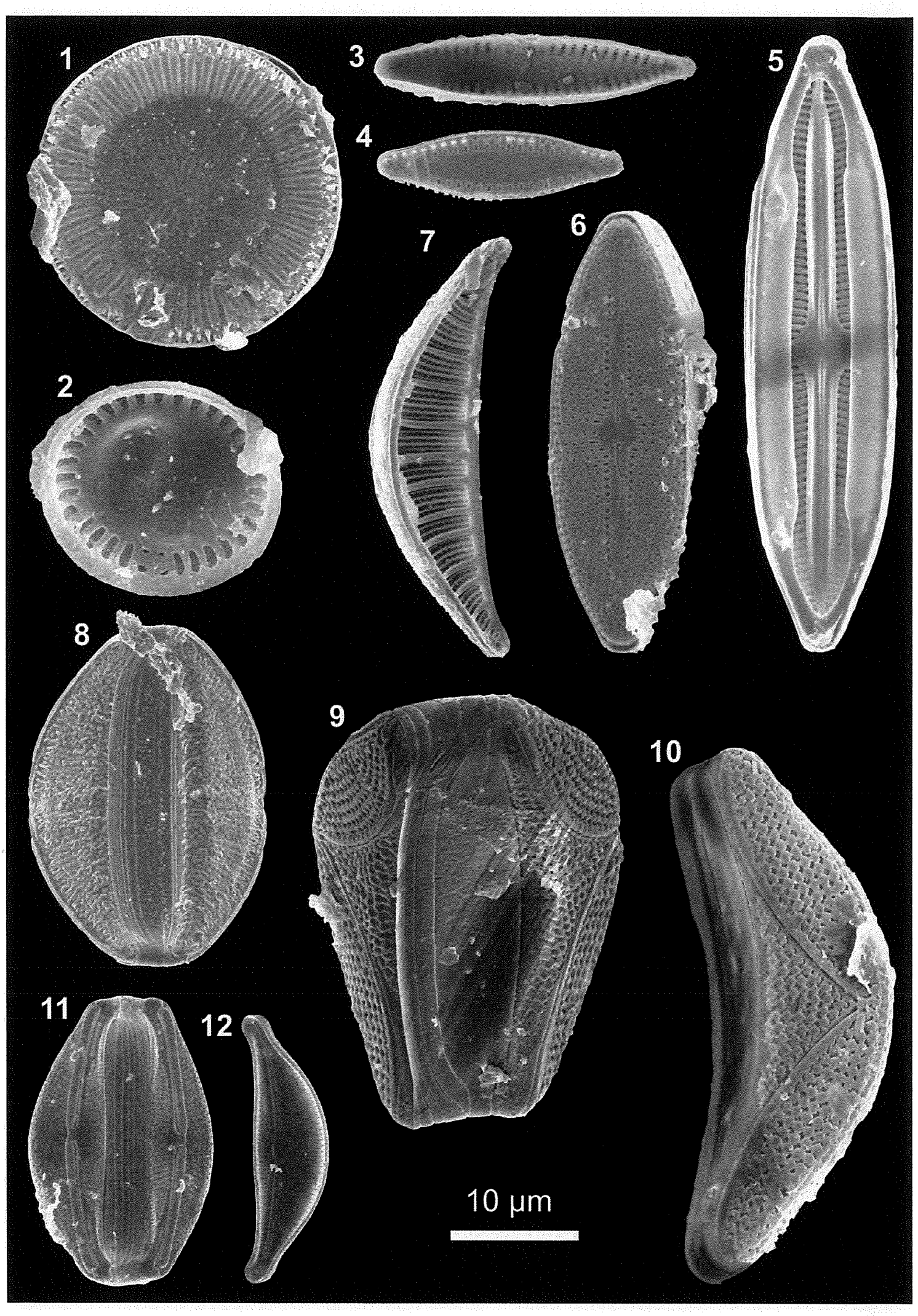
1
3
4
5
2
7
6
8
9
10
11
12
10 µm

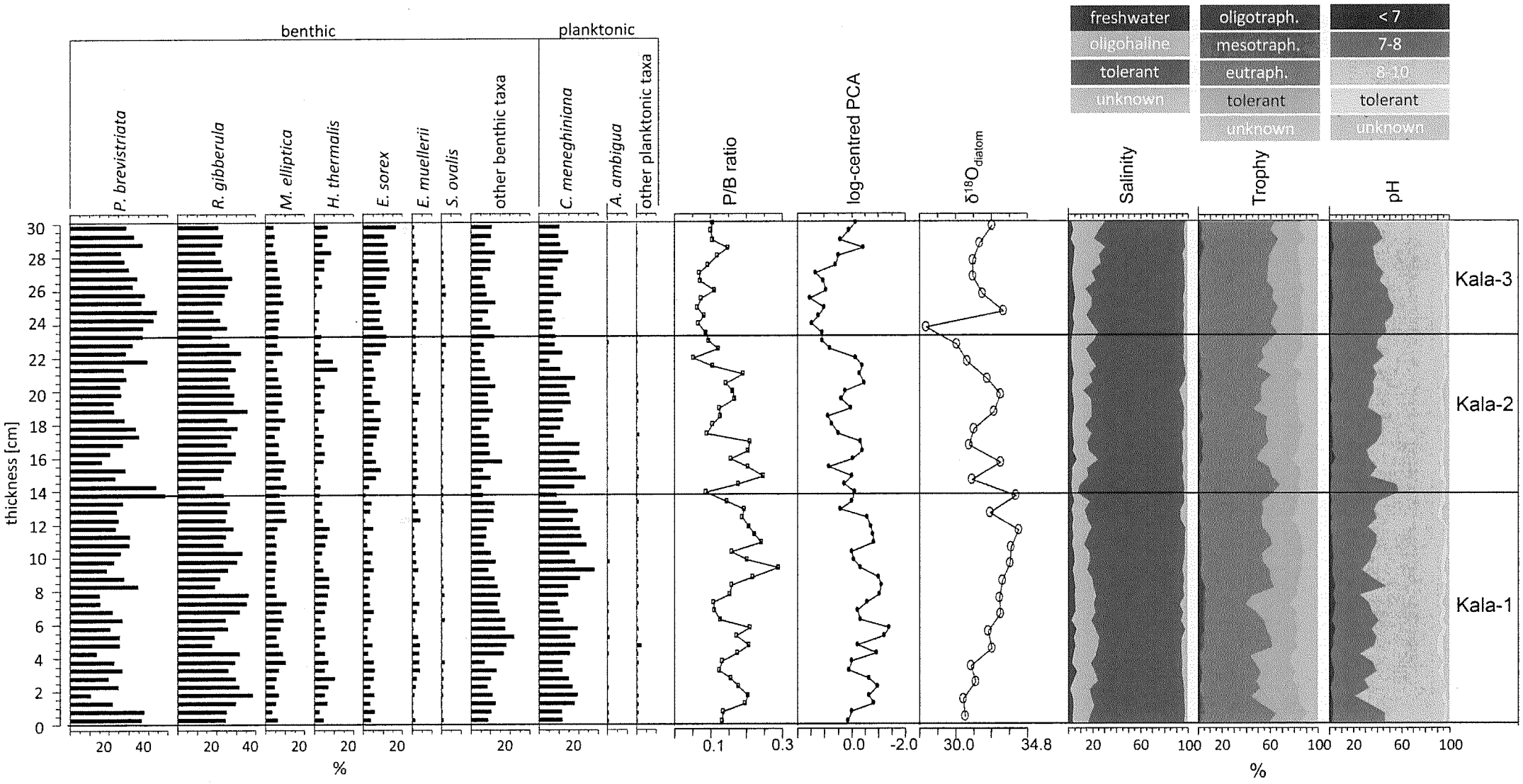
benthic
planktonic
P. brevistriata
R. gibberula
M. elliptica
H. thermalis
E. sorex
E. muellerii
S. ovalis
other benthic taxa
C. meneghiniana
A. ambigua
other planktonic taxa
P/B ratio
log-centred PCA
δ18Odiatom
Salinity
Trophy
pH
freshwater
oligohaline
tolerant
unknown
oligotraph.
mesotraph.
eutraph.
tolerant
unknown
< 7
7-8
8-10
tolerant
unknown
thickness [cm]
Kala-3
Kala-2
Kala-1
%
%

Table 1 Analytical data for OSL age calculation: Sample code, ^{238}U, ^{232}Th and ^{40}K-concentrations, total dose rate, equivalent dose and OSL age

Sample	U [ppm]	Th [ppm]	K [%]	$\dot{D}$ [Gy/ka]	D_e [Gy]	OSL Age [ka]
BT 885	1.14 ± 0.08	2.20 ± 0.05	0.41 ± 0.01	0.88 ± 0.04	77.6 ± 3.8	88.5 ± 5.8
BT 1052	0.97 ± 010	2.02 ± 0.04	0.32 ± 0.01	0.66 ± 0.03	59.7 ± 5.2	90.3 ± 9.2
BT 1054	0.91 ± 0.07	2.38 ± 0.05	0.34 ± 0.01	0.69 ± 0.33	72.9 ± 3.7	106.3 ± 7.4
BT 1055	0.93 ± 0.09	2.42 ± 0.05	0.33 ± 0.01	0.68 ± 0.33	70.7 ± 2.8	103.4 ± 6.4